REPORT DOCUMENTATION PAGE

AFRL-SR-BL-TR-98-

0737

1. AGENCY USE ONLY (Leave Blank)	2. REPORT DATE	3. REPC
	None Shown	Final

4. TITLE AND SUBTITLE
Measurement of the Diffusion Coefficient of Strongly Interacting Colloidal Suspensions by Nondegenerate Two-Wave Mixing

5. FUNDING NUMBERS

6. AUTHORS
C. L. Adler and N. M. Lawandy

7. PERFORMING ORGANIZATION NAME(S) AND ADDRESS(ES)
Brown University

8. PERFORMING ORGANIZATION REPORT NUMBER

9. SPONSORING/MONITORING AGENCY NAME(S) AND ADDRESS(ES)
AFOSR/NI
4040 Fairfax Dr, Suite 500
Arlington, VA 22203-1613

10. SPONSORING/MONITORING AGENCY REPORT NUMBER

11. SUPPLEMENTARY NOTES

12a. DISTRIBUTION AVAILABILITY STATEMENT
Approved for Public Release

12b. DISTRIBUTION CODE

13. ABSTRACT *(Maximum 200 words)*
See Attachment

19981202030

14. SUBJECT TERMS	15. NUMBER OF PAGES
	16. PRICE CODE

17. SECURITY CLASSIFICATION OF REPORT	18. SECURITY CLASSIFICATION OF THIS PAGE	19. SECURITY CLASSIFICATION OF ABSTRACT	20. LIMITATION OF ABSTRACT
Unclassified	Unclassified	Unclassified	UL

Measurement of the diffusion coefficient of strongly interacting colloidal suspensions by nondegenerate two- wave mixing

by

C. L. Adler* and N.M. Lawandy†

*Department of Physics
†Division of Engineering and Department of Physics

Brown University
Providence, RI

We have measured the diffusion coefficient of strongly interacting "colloidal liquids" near the "liquid"-"solid" phase transition using nondegenerate two-wave mixing. We self-consistently calculate the diffusion coefficient as the product of the elastic modulus and a relaxation time which is identified as the time taken for a particle to diffuse one-tenth of the average interparticle distance. This procedure also predicts an electrolyte concentration where the diffusion coefficient vanishes which is identified with the melting point of the colloidal crystal. This is shown to be essentially identical to the Lindemann criterion. In addition, we findthat the colloidal liquid-solid transition as a function of ionic concentration gives a critical exponent $\gamma=0.08\pm0.003$.

Suspensions of charged polystyrene microspheres have received intense interest in recent years because of the discovery that they could form ordered crystalline phases in ultraclean water which could be investigated using quasi-elastic light scattering methods.[1] The crystals are thought to be purely repulsive and easily melt upon the addition of small amounts of salts which screen the interactions of the charges on the particle surfaces. The particles interact through a Debye potential with the strength of the potential characterized by the number of charges per microsphere and the strength of ionic concentration in the suspension.[1,2,3] As such, the suspensions can be well characterized, and form model systems for studying some basic condensed matter physics.

The crystals have had many applications in pure and applied physics. Due to their strong reflectance at the Bragg condition, they have been proposed for Raman filters [4], DFB lasers [5], and as model systems for the study of the inhibition of spontaneous emission[6]. In addition, the non-crystalline colloidal suspensions have an extremely high nonlinear index of refraction based on the ponderomotive force [7,8]. These "artificial Kerr media" have nonlinearities 10^5 times that of CS_2 with relaxation times on the order of milliseconds. Self-focusing, self-trapping, and degenerate four-wave mixing have been observed due to the high nonlinear index. [7,8].

Because they can be well characterized, there have been many experimental and theoretical studies performed to determine their properties. Studies of the polyballs have observed the iridescence of the structured phase at the freezing point[9] and measured the viscosity by monitoring the decay of absorption gratings in tagged particles[10] and correlated light scattering experiments [11]. Other work has observed the onset of dilitancy in noninteracting systems[12], and measured Young's modulus by the change in lattice spacing under gravitational compression[13] and the resonance frequency of standing shear modes.[14] Theoretical studies have used the Lindemann criterion[15]and effective hard-sphere radii[16]

to determine the melting point. Other theoretical studies of nonequilibrium properties of these systems have calculated viscosities using the Smoluchowski equation[17], the structure factor of the colloidal liquid [18], and arguments based on effective relaxation times of the strongly interacting system [19].

Our work concerns the use of the high nonlinear index for investigation of the properties of the strongly interacting colloid. We have developed a technique which measures the absolute low-shear-rate viscosity of solutions to within ten percent of previously tabulated values with sample volumes as small as 20 picoliters. This technique relies on the forces associated with radiation pressure in a travelling optical intensity grating. It is based on the exchange of energy between the two interfering light beams mediated by colloidal medium, referred to as nondegenerate two-wave mixing (NDTWM). We have then predicted the effective viscosities using a relaxation-time argument originally given in reference 19, and found them to match our experimental work to about 10%.

Theory of NDTWM in Colloids

A dielectric particle within these suspensions will feel a force exerted on it in a light field with a strong intensity gradient in the direction of the gradient. The force is given by the expression[7,8]

$$F = \frac{\alpha}{c} \nabla I \qquad (1)$$

where α is the polarizability of the particle, I the intensity of the light field as a function of the spatial coordinates, and c the speed of light. The polarizability is given by

$$\alpha = 4\pi \frac{n^2-1}{n^2+2} a^3 \qquad \text{(MKSA units)} \qquad (2)$$

a being the radius of the particle (430 Å in this work) and n being the ratio of the indices of refraction of polystyrene and water. Nonlinear effects in these artificial Kerr media are caused by the change in the net index of refraction due to changes in the colloidal particle number density from the gradient force, as it can be shown that the effective index of refraction of the composite medium is linearly proportional to the volume fraction of the polystyrene microspheres.[4,7,8] We are interested in the effects caused by a moving index grating from the interference of two Doppler shifted light beams. The effect was first seen in 1986 by Chang and Sato[20], and studied theoretically by McGraw and Rogovin in 1987.[21]

When two counter-propagating Doppler-shifted light beams are superposed in a nonlinear medium, the travelling intensity grating that results will lead to a travelling index grating. This in turn leads to the scattering of one light beam into the direction of the other, indicating that one beam will gain energy at the expense of the other one. For low intensities, the NDTWM gain is given by [21]

$$G \sim \frac{\delta\omega\tau}{1+(\delta\omega\tau)^2} \qquad (3)$$

where $\frac{1}{\tau} = 4k^2D$, $k = \frac{2\pi}{\lambda}$, and D is the diffusion coefficient of the particle. Expression (3) allows the diffusion coefficient to be measured directly by measuring the NDTWM gain curve as a function of $\delta\omega$. At higher intensities, the peak of the gain curve is a function of g, which is a dimensionless ratio proportional to $\frac{I}{ck_bT}$, the ratio of the potential the colloidal particle sits in to the mean thermal energy. Figure 1 shows several normalized gain curves at differing values of g.

Dozier *et al.*[10] make an important distinction between two different types of diffusion coefficient. There is the single particle D_0 which is a measure of the average single-particle displacement in a time t:

$$\langle x^2 \rangle = \frac{t}{3D} \qquad 4$$

and the mutual diffusion coefficeient D_k which indicates how a density modulation of wavevector k will decay through diffusion:

$$D_k \nabla \rho_k = - \frac{\partial \rho_K}{\partial t} \qquad 5$$

These are only neccessarily the same for noninteracting particles. In the derivation of NDTWM in reference 21, it is obvious that the mutual diffusion coefficient is what is being measured by NDTWM. However, the wavelength of light which we are using is λ=0.514 μm. Multiple particle effects ought to come in only if there are many particles per "cubic wavelength".

An estimate of the number of particles per cubic wavelength being dragged along in the travelling-wave graing is $N \sim 4\pi/3\ (\lambda/2n)^3 \rho \sim 10$ particles. Therefore, although in theory what we are measuring is the mutual diffusion coefficient, in practice we believe that what we measure should essentially be the single particle value.

Experimental Measurement of the Diffusion Coefficient

Figure 2 shows our experimental setup. The laser used was a 5 W argon-ion laser running at 514.5 nm. The PZT was driven using a triangle wave signal at 200 Hz, and the output from the detectors was lock-in detected using as reference an attenuated signal from the function generator driving the PZT. Phase sensitive detection at the PZT displacement frequency insured that we only detected gain antisymmetric in the beam Doppler shift. PZT displacement was calibrated by Michelson interferometry. The diameter of the beam going through the microscope objectives was measured to be approximately 7 μm by measuring the power transmitted through pinholes of different sizes. The sample holder was a 275 μm thick 5 microliter volume pipette, from which the sample volume probed is estimated to be approximately 2×10^{-8} cm^3, or 20 picoliters.

A scope trace of the output from detector 1 is shown in figure 3. The upper trace is proportional to the PZT displacement; the lower is the NDTWM signal. Output from detectors 1 and 2 is shown in figure 4, showing that one beam gains energy at the expense of the other. Figure 5 shows NDTWM signal as a function of beam Doppler shift, showing that the gain curve is lorentzian.

The peak of the gain curve shifted to higher frequencies as the laser power was increased (fig 6). However, estimates show that $g \ll 1$ at all laser powers, which indicates that the doppler shift giving the peak gain should not change due to McGraw and Rogovin's theory. But a simple calculation based on the estimated value of the nonlinear index, $n_2 = 4 \times 10^{-11}$ m^2/W, indicated that the threshold for self-focusing was approximately 20 mW. Computer solution of the nonlinear wave equation using a code developed at our

laboratory[22] showed that self-focusing effects led to intensity increases at the center of the beam which would increase g to the values needed to see this peak shift. (Figure 7). We took great care to insure that all later experiments were performed with powers under the self-focusing threshold.

The apparatus was calibrated against suspensions of noninteracting colloids whose viscosity could be calculated from the Handbook of Chemistry and Physics. The three solutions were 2/3 by volume aqueous suspensions of 10% by volume 0.090 μm diameter polystyrene microspheres and 1/3 by volume mixtures of glycerol and water. We used three mixtures to test our apparatus, which were pure water, 1/2 water and 1/2 glycerol, and pure glycerol. The NDTWM gain from these three colloidal suspensions is shown in figure 8, from which it can be seen that the position of the peak changes by over a factor of two with increasing viscosity. Using the relationship given in formula 3 and Stokes' law (formula 13b), the absolute viscosity is calculated to be within 10% of the value given by the Handbook of Chemistry and Physics at all three concentrations [23].

The experiments on strongly interacting colloids were performed on 0.086 μm diameter microspheres from Interfacial Dynamics Corporation (IDC). From IDC literature, the surface charge density on the polystyrene microspheres was 1 charge/2500 $Å^2$, leading to a total charge of roughly 900 e^- per sphere. The colloidal suspensions were crystallized by agitating solutions with ion-exchange resin (Dow Chemical Mixed-Bed Analytic Resin) which lowered the electrolyte concentration to at most 10^{-6} Molar, at which point a solution of NaCl in water was added to raise the ionic strength to well defined values. Below an electrolyte concentration of 1.6×10^{-4} Molar no measurable signal could be seen. The frequency detuning of the peak of the gain curve for full bottle concentration (volume fraction (ϕ) = 0.1) is plotted in figure 9. This figure shows that at low salt concentrations, the diffusion coefficient is very low, but rises rapidly with increasing electrolyte concentration.

We believed that the change in the diffusion coefficient was due to the melting of the colloidal crystal, as in the work of Dozier *et al.*[10]. However, we could not directly see the melting transition because the Bragg notch was located in the near UV. To test this idea, we measured the transmissivity of a series of colloidal suspensions at differing NaCl concentrations. The suspensions were made up in standard 100 μm thick cuvettes, and their transmissivity was measured on a Cary spectrometer. Figure 10 shows the transmissivity in the 300-500 nm region of the spectrum. Curve a and b (at 0 and 10^{-4} M NaCl concentration) have clearly defined "notches" near 390 nm due to Bragg scattering of these wavelengths, characteristic of long-range order in the suspension. Curves c and d (at 1.4 and 2 x10^{-4} M) show no diffraction minimum, indicating that at or near 1.4x10^{-4} M the colloidal crystal "melted", which is near the concentration where the diffusion coefficient becomes zero from extrapolation of the data in figure 9.

Theory of the Melting Transition of the Colloidal Crystal

The phase transition observed is probably an example of a Kirkwood-Alder transition [24,25]. In 1939, Kirkwood predicted that a hard-sphere liquid would undergo a transition to long-range order when the packing fraction of the hard spheres exceeded a certain value which was significantly less than the close-packing limit of 0.74. Computer experiments subsequently demonstrated that the packing fraction for crystallization is of the order of 0.55-0.6 [25]. Related work (mentioned above) demonstrated that the experimental onset of dilitancy in a hard-sphere system (where percolation causes large-scale structures in the system) occurs around a packing fraction of 0.55, which is probably related to the establishment of long-range order [13].

The colloidal suspensions which we work with are not simple hard spheres. They are polystyrene beads with a measured charge of roughly 900 e^- per sphere. Any discussion of the melting transition has to take this into account. There has been work done on assigning effective hard-sphere radii to the spheres based on the interparticle potential,treating the transition as a Kirkwood transition when the effective packing fraction

reaches 0.55.[26] We discuss the phase transition in a different, but related, manner, namely assuming that the crystal phase exists and using the Lindemann criterion for determining when thermal fluctuations will destroy long-range order.[27]

The colloidal suspensions are composed of hard charged spheres surrounded by a "fluid" of counterions. The counterions are of two types: those that detached from the polystyrene spheres when originally made, and those added by the experimenters. The suspension is net charge neutral. The interparticle potential is a solution to the Poisson-Boltzmann equation:

$$-\nabla^2\phi = \frac{\rho}{\varepsilon} \qquad 6\,a$$

$$\rho = en \sinh(e\phi/k_bT) + Zeq \exp(Ze\phi/k_bT) \qquad 6\,b$$

This assumes a colloid with added univalent electrolye of density n and polystyrene microspheres of density q with Z charges per microsphere.

Linearizing the equation leads to solutions for the potential around a polyball with the assumption that the field must approach that of a point charge of charge Ze as the density of screening ions goes to zero:

$$U(r) = Ze\,\phi = \frac{(Ze)^2}{4\pi\varepsilon\varepsilon_0 r}\,\frac{\exp(-\kappa(r-2a))}{1+\kappa a} \qquad 7$$

$$\kappa^2 = \frac{e^2(2n+Zq)}{\varepsilon\varepsilon_0 k_bT} \qquad 8$$

The Debye screening length, $1/\kappa$, is a measure of the extent of the potential which drops off as the electrolyte concentration is increased .

The form of the potential given by equation 7 is not universally accepted. U(r) is given by the solution of a nonlinear PDE, and should not be expected to be valid outside of the limit $\kappa q^{-1/3} \leq 1$ (that is, the low concentration limit). There is some evidence for an attractive potential in the paper by Ise et al, who saw an increase in the crystal plane spacing with increasing counterion concentration.[29] The lattice spacing for a purely repulsive crystal is dictated by purely geometric considerations. Interestingly enough, we saw the same general behavior (increase in lattice spacing with increasing salt) from the transmittivity experiments, although any inference based on two points of data is extremely weak. To the best of our knowledge, the true form of the interparticle potential has not been determined. We will show in this paper that the purely-repulsive potential given in equation 7 predicts the observed melting point using the Lindemann criterion relatively accurately, and also predicts the diffusion coefficient for the colloidal "liquid" when using a relaxation-time approximation based on the one given in reference 19.

We assume that the particles form a colloidal crystal with simple cubic structure to simplify calculation. Other assumptions will only change the results below by factors close to unity. Assuming that the colloidal particles are separated by an average distance $\langle d \rangle = (1/q)^{1/3}$, the potential on a microsphere at a position d between two infinite planes of spheres separated by a distance $2\langle d \rangle$ can be expanded out to second order in $\delta = |d - \langle d \rangle|$. This leads to

$$U_i = \frac{Z^2 e^2}{2\varepsilon \langle d \rangle^3} \frac{\exp(-\kappa(\langle d \rangle - a))}{1+\kappa a} (\kappa \langle d \rangle)\, \delta^2 = \frac{1}{2} k\, \delta^2 \qquad 9$$

By expanding to second order about the potential minimum, we derive an effective "spring constant", k, for this system. The Lindemann criterion for the melting point states that the melting transition for a crystal occurs when thermal energy causes the average displacement of a particle from its equilibrium position by about 10% of the lattice spacing of the crystal.

Assuming that each mode has average energy $1/2k_bT$, we arrive at the transcendental equation

$$\kappa(<d>-2a) = \ln\left(\frac{0.01\ Z^2e^2\kappa}{2\varepsilon k_bT(1+\kappa a)}\right) \qquad 10$$

We will assume that $\frac{\kappa}{1+\kappa a} \sim \frac{1}{a}$ to avoid having to solve the transcendental equation. It can be shown that inclusion of this factor can change the value of κ obtained by at most 10-20 % because of the slow variation of the logarithm with the size of its arguments.

$$\kappa = \frac{1}{<d>-a}\ln\left(\frac{0.01\ Z^2e^2}{2\varepsilon a k_bT}\right) \qquad 11$$

To simplify notation, we define a dimensionless measure of the strength of the potential, γ.

$$\gamma = \frac{Z^2e^2}{2\varepsilon a k_bT} \qquad 12$$

Using $Z \approx 900$ e^- /polyball with radius a=0.043 μm and volume fraction ϕ=10%, we calculate $\gamma=1.12\times10^4$. Figure 12 is a plot of the electrolyte concentration necessary to melt the colloidal crystal as a function of the volume fraction of the suspension. As can be seen, for $\phi = 0.1$ it predicts a salt concentration of about 1.6×10^{-4} M. To test the validity of this expression, we measured the electrolyte concentration neccessary to melt a colloidal crystal with ϕ=0.02. At this concentration, the condition for Bragg scattering is satisfied by light with a wavelength around 6000 Å, which gives the crystal a brilliant irridescence. We measured the electrolyte concentration necessary to melt the crystal by finding the concentration where the irridescence vanished. The melting point was between 10^{-5} and 2×10^{-5} M NaCl, whereas the Lindemann theory predicts 7×10^{-6} M.

Reference 19 presents a theory which predicts the viscosity of colloidal suspensions in regimes far from the melting transition. The viscosity η can be expressed as $\eta = G\tau$ where τ is a relaxation time dependent only on the mean separation of particles, and G is the bulk modulus for the system. In reference 19, τ is assumed to be the time for a particle to diffuse a distance $\langle d \rangle/\beta$ where β is on the order of 10:

$$\tau \sim \frac{\langle d \rangle^2}{\beta^2} D \qquad 13a$$

$$D = \frac{k_b T}{6\pi\eta a} \qquad 13b$$

Equation 13b relating the viscosity to the diffusion coefficient is Stokes' law. In reference 19, η was taken as the viscosity of water, but we will show that if the viscosity is defined self-consistently, the diffusion coefficient will go to zero at a nonzero electrolyte concentration and that this concentration is essentially the concentration at which the solid-liquid phase transition is predicted by the Lindemann criterion. We approximate the bulk modulus, G, by $k/\langle d \rangle$ where k is the "spring constant" defined in equation 9 above.

The viscosity of the suspension is $\eta_T = \eta_0 + \eta$, where η_T is the total overall viscosity, η_0 is the viscosity of water, and η is the viscosity due to the interaction of the charged colloidal particles.[19] From equations 13a and b, we arrive at an expression for η:

$$\eta = G(\frac{d}{10})^2/D = \frac{6\pi\eta_T a}{k_b T} G \frac{d^2}{\beta^2} \qquad 14$$

Expressing η in terms of the viscosity of water leads to:

$$\eta = \eta_0 (\frac{Q}{1-Q}), \qquad Q<1 \qquad 15$$

where $Q = \frac{6\pi a G d^2}{k_b T \beta^2}$. Adding the viscosity of water to the viscosity due to the colloidal suspension, the total viscosity is

$$\eta_T = \frac{1}{1-Q}\eta_0 \qquad 16$$

Using Stokes' law, we can write the diffusion coefficient in terms of D_0, the diffusion coefficient of a colloidal particle in the absence of interactions, as:

$$\frac{D}{D_0} = 1-Q \qquad Q<1 \qquad 17a$$

$$\frac{D}{D_0} = 0 \qquad Q\geq 1 \qquad 17b$$

At Q=1 the single particle diffusion coefficient vanishes, indicating a liquid-solid phase transition. In fact, Q = 1 corresponds to the Lindemann criterion, as we show below.

We estimated that G = k/<d> where k was given by equation 7. Setting Q=1 we arrive at an expression estimating the value of k where the diffusion coefficient vanishes:

$$6\pi k \left(\frac{a}{d}\right)\left(\frac{d}{\beta}\right)^2 = k_b T \qquad 18$$

As $6\pi \frac{a}{d} \sim 1$ and β has been taken to be on the order of 10, this is the Lindemann criterion. Equation 17 is compared to the measured diffusion coefficent in figure 12, with β=14 chosen to best fit the experimental data. This value of β also fits the melting point of the lower-density crystal as well.

We have applied this theory to the data in the paper by Dozier et al.[10] which is given in the same format as our data. This is an ideal test of this theory, as their concentration regime is an order of magnitude below ours (ϕ=0.01). From their quoted

value of 300 charges per polyball, $\gamma = 550$, which is again an order of magnitude below that of our samples. Figure 13 is a plot of D/D_0 taken from reference 10 compared to equation 17 with $\beta=14$ again. As can be seen, agreement is quite good in both predicting the electrolyte concentration where their suspension solidifies, and in predicting the single-particle diffusivity beyond the melting point.

The experimental results were further fit to a critical parameter relation in order to establish a critical exponent. We assumed that $D/D_0 \sim (n-n_T)^{\alpha}$, where n is the electrolyte concentration, n_T the concentration at the transition point, and α the critical exponent characterizing the phase transition. The best fit was obtained with $\alpha = 0.08$, with a margin of error of 0.003 and $n_T = 1.6 \pm 0.1 \times 10^{-4}$ M/l. Figure 14 shows that the power law behavior fits the experimentally obtained diffusivity near the melting point.

We have shown using two-wave mixing and light scattering data, that a large change in the diffusivity of colloidal particles takes place near the order-disorder transition in a colloidal suspension. The single-particle diffusivities measured in the colloidal "liquid" are predicted reasonably accurately using a bulk modulus derived from the Debye potential and a relaxation time derived by defining the viscosity self-consistently. The model is of interest as it predicts an electrolyte concentration where the diffusion coefficient becomes zero, which is identified as the point at which the colloidal crystal melts. This concentration is identical to the melting point predicted by the Lindemann criterion.

Acknowledgements

One of us (CLA) would like to acknowledge the support of a UES Air Force Graduate Fellowship (contract F49620-86-C-0127). We would both like to thank John Moon for his help in using the Cary spectrometer, and Professor Edward Mason for several informative talks.

References

1. P.A. Hiltner and I. M. Krieger, J. Phys. Chem., 73, 2386 (1969)

2. P. Pieranski, Contemp. Physics, **24** , 25 (1983)

3. N. A. Clark, A. J. Hurd, and B. J. Ackerson, Nature, 281, 57 (1979)

4. S.A. Asher, P. L. Flaugh, and G. Washinger, Spectroscopy, 1, 26 (1986)

5. J. Martorell and N.M. Lawandy,"Distributed Feedback Oscillation in Ordered Colloidal Suspensions of Polystyrene Microspheres" in *International Conference on Quantum Electronics Technical Digest Series 1990, Vol. 8* (Optical Society of America, Washington, DC, 1990) p. 176; also, accepted to Optics Communications under that title

6. J. Martorell and N.M. Lawandy, "Observation of Inhibited Spontaneous Emission in 3-D Periodic Bragg Structures" in *International Conference on Quantum Electronics Technical Digest Series 1990, Vol. 8* (Optical Society of America, Washington, DC, 1990) p. 136; also, accepted by Phys. Rev. Letters under the same title

7. A. Ashkin, J. M. Dziedzic and P.W. Smith, Optics Letters, 7 , 276 (1982)

8. Smith, P.W., Maloney, P.J., and Ashkin, A., Optics Letters, 7, 347 (1982)

9. D. J. W. Aastuen, N. A. Clark, L.K. Cotter, and B. J. Ackerson, Phys. Rev Lett.,57,1733 (1986)

10. W.D. Dozier, H.M. Lindsay and P.M. Chaikin, J. Phys. Coll., 46 , C3-165 (1985)

11.J. C. Brown, P.N. Pusey, J.W. Goodwing, and R.H. Ottewill, J. Phys. A, 8, 664 (1975)

14. H.M. Lindsay and P.M. Chaikin, J. Chem. Phys., 76,3774 (1982)

12. G. Y. Onoda and E. G. Liniger, Phys. Rev. Lett., 64,2727 (1990)

13. R.S. Crandall and R. Williams, Science, 198, 293 (1977)

15. D. Hone, S. Alexander, P. M. Chaikin, and P. Pincus, J. Chem Phys., 79,1474 (1983)

16. W. -H. Shih and D. Stroud, J. Chem. Phys., 79, 6254 (1983)

17. B.J. Ackerson, J. Chem. Phys., 64, 242 (1976)

18. D. Ronis, Phys. Rev. A., 34,1472 (1986)

19. H.M. Lindsay, W.D. Dozier, P.M. Chaikin, R. Klein, and W. Hess, J. Phys. A,19,2583 (1986)

20. S. Chang and T. Sato , Appl. Optics, 25,1634 (1986)

21. R. McGraw and D. Rogovin, Phys. Rev. A, 35,1181 (1987)

22. R.S. Afzal, N.M. Lawandy and W.P. Lin, JOSA B, 6,2348 (1989)

23. This work has been accepted by Optics Communications under the title "Viscosity of Picoliter Volumes Measured by Nondegenerate Two-Wave Mixing", C.L. Adler and N.M. Lawandy.

24. J.G. Kirkwood, J. Chem. Phys. 7,919 (1939)

25. B.E. Alder and T.E. Wainwright, Phys. Rev., 127,359 (1962)

26. C.S. Hirtzel and R. Rajagopalan, Colloidal Phenomena, Noyes Publications (New Jersey, 1985) pp.174-178; see also ref. 16

27. P.A. Forsyth, J.S. Marcelja, D.J. Mitchell, and B.W. Ninham, Adv. Coll. Int. Sci., 89, 574 (1982); see also ref. 15

28. J.G. Kirkwood, Chem. Rev., 19,275 (1936)

29. N. Ise, T. Okubo, M. Sugimura, K. Ito, and N.H. Nolte, J. Chem. Phys 78,536 (1983)

Figure Captions

Figure 1 NDTWM gain as a function of g. Gain is normalized by $\frac{1}{\rho g}$. (After ref. 5)

Figure 2 Experimental setup. B is a 50/50 beamsplitter, PZT is a mirror mounted on a piezoelectric transducer, M are 10x microscope objectives, and P is the sample holder, a 5 microliter volume pipette.

Figure 3 Scope trace of NDTWM gain. The upper trace is the ramp voltage for the PZT; the lower is signal from detector 1. As gain is dependent on beam doppler shift, the lower trace should look like the derivative of the upper. The time scale is 1 ms/div; the top voltage scale is 1 V/div, and the bottom is 5 mV/div.

Figure 4 Top trace: detector 1 signal. Bottom trace: detector 2. Time scale is 2 ms/div.

Figure 5 NDTWM gain as a function of beam doppler shift

Figure 6 Dependence of the peak of the gain curve on laser power

Figure 7 Two wave mixing gain in three solutions.

The solutions were 2/3 0.090 μm microspheres in deionized water with

a) 1/3 water

b) 1/6 water, 1/6 glycerol

c)1/3 glycerol

Figure 8 Normalized frequency of peak gain vs. g

a) From McGraw and Rogovin's theory (ref. 5)

b) Calculated from self-focusing model and experiment (cf. fig. 6)

Figure 9 Normalized diffusion coefficient of 0.086 μm diameter polystyrene microspheres as a function of NaCl concentration (ϕ=0.10)

Figure 10 Transmission spectra of colloidal crystal

NaCl concentration

a) 0 M/l

b) 1.0×10^{-4} M/l

c) 1.4×10^{-4} M/l

d) 2.0×10^{-4} M/l

Figure 11 Theoretical melting concentration of colloidal crystal as a function of volume fraction

Figure 12 Theoretical diffusion coefficient compared to experimental value;
ϕ=0.1, $\gamma=1.12 \times 10^4$

Figure 13 Theoretical diffusion coefficient compared to actual value (data from reference 10) ϕ=0.01, $\gamma=5.50 \times 10^2$

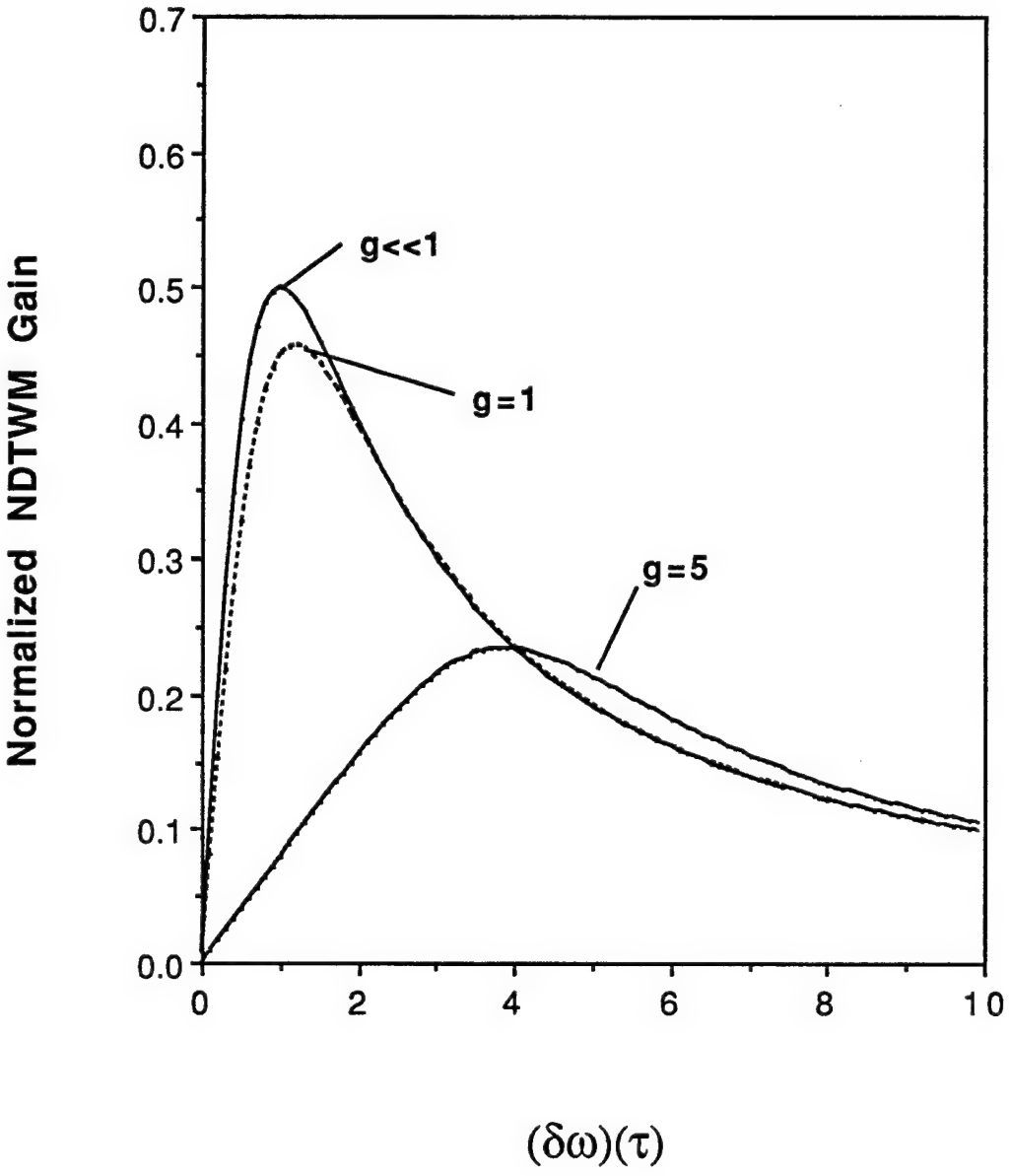
Normalized NDTWM Gain
0.7
0.6
0.5
0.4
0.3
0.2
0.1
0.0
0
2
4
6
8
10
g<<1
g=1
g=5
(δω)(τ)

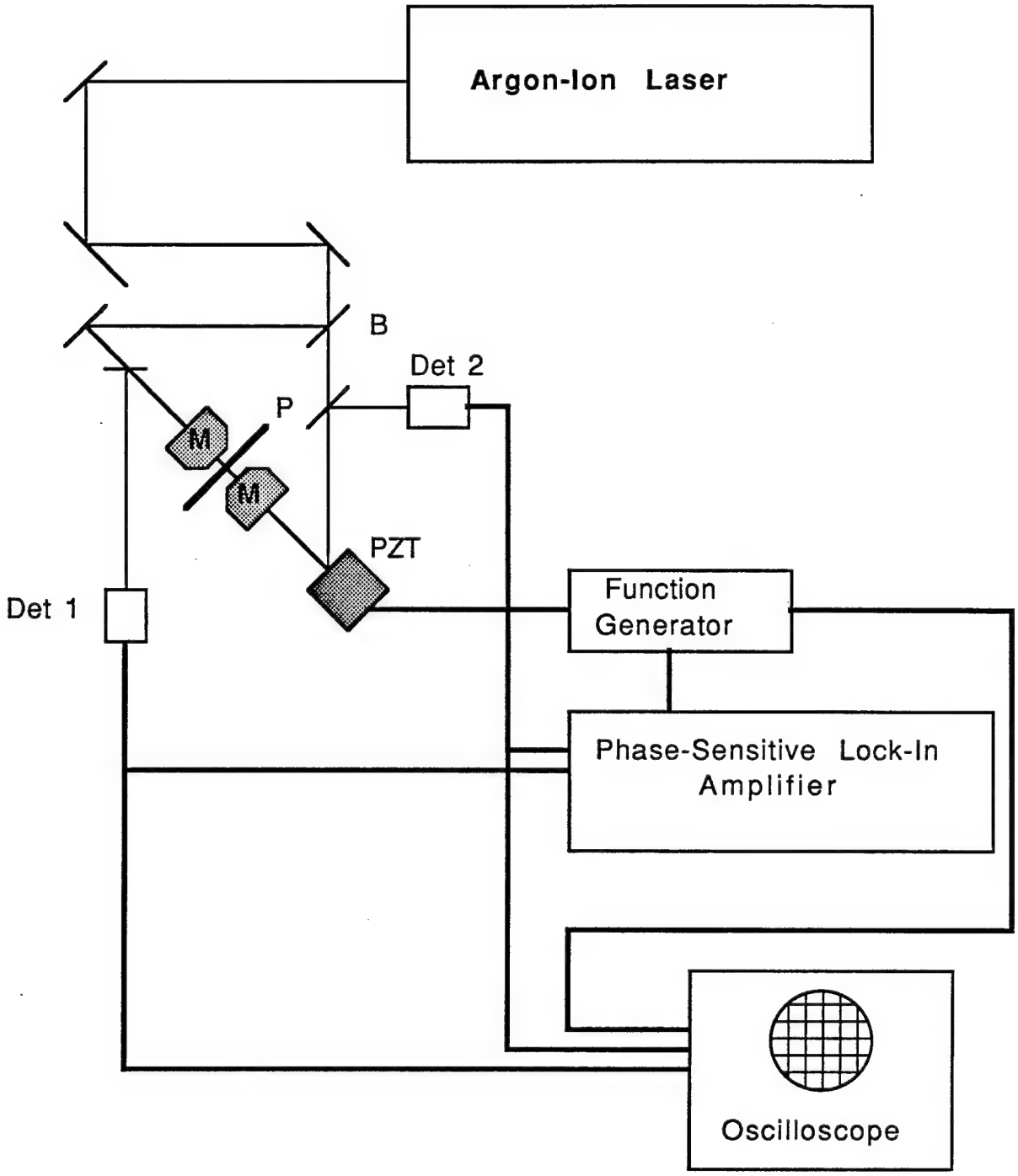
Argon-Ion Laser
B
Det 2
P
M
M
PZT
Det 1
Function Generator
Phase-Sensitive Lock-In Amplifier
Oscilloscope

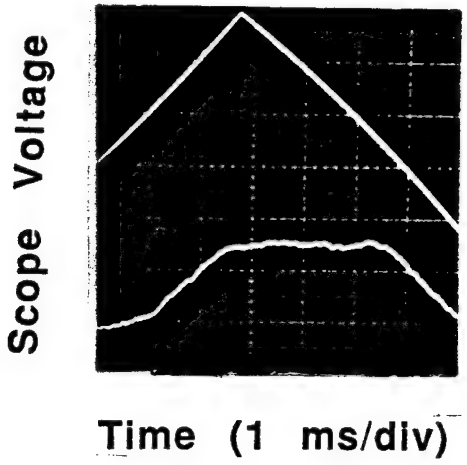
Scope Voltage
Time (1 ms/div)

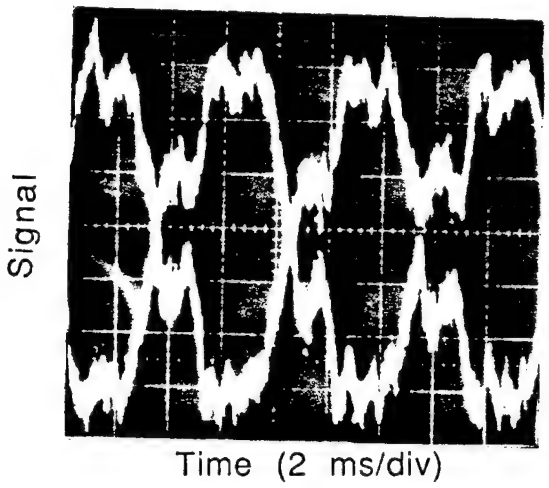
Signal
Time (2 ms/div)

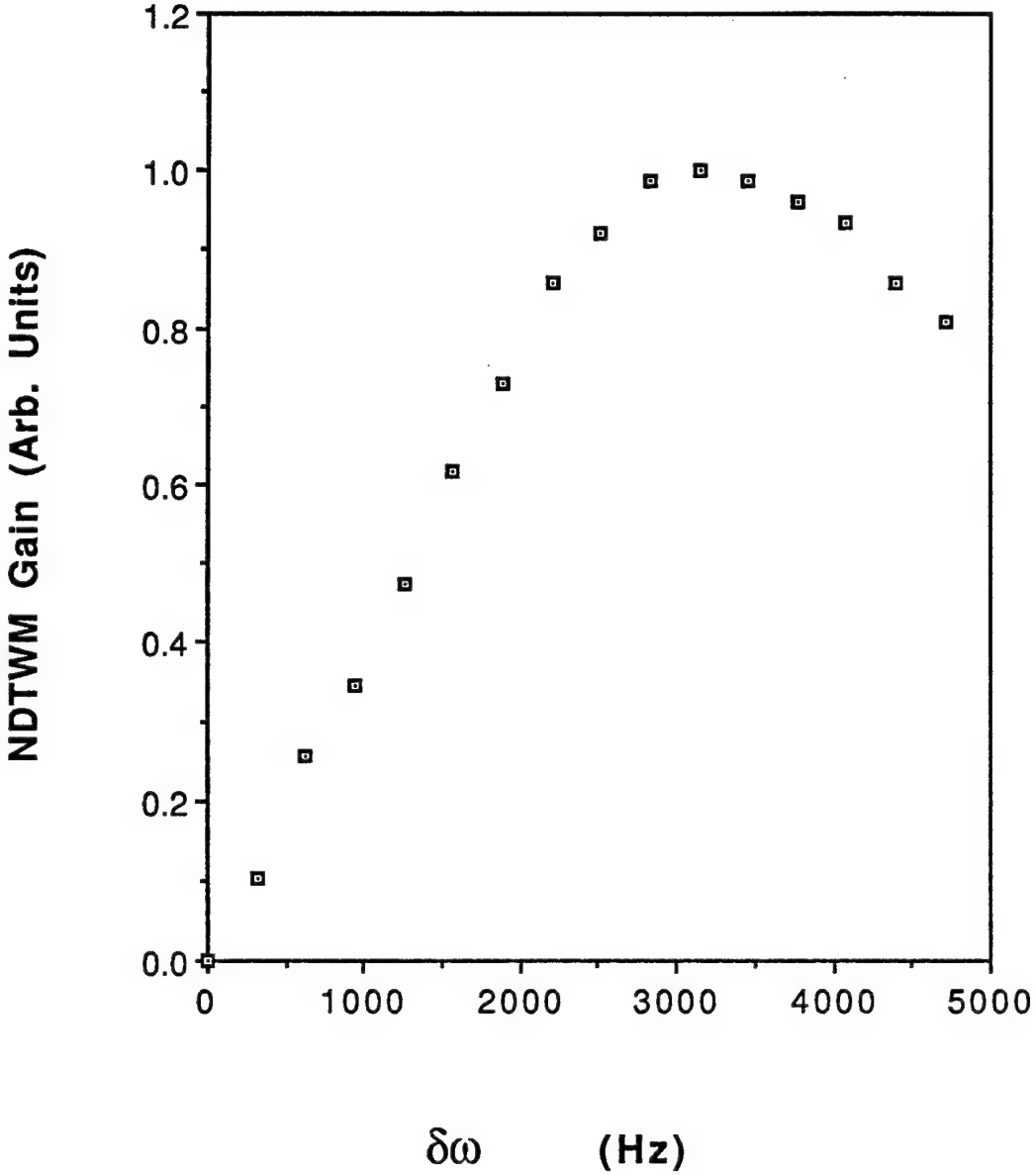
NDTWM Gain (Arb. Units)
1.2
1.0
0.8
0.6
0.4
0.2
0.0
0
1000
2000
3000
4000
5000
δω (Hz)

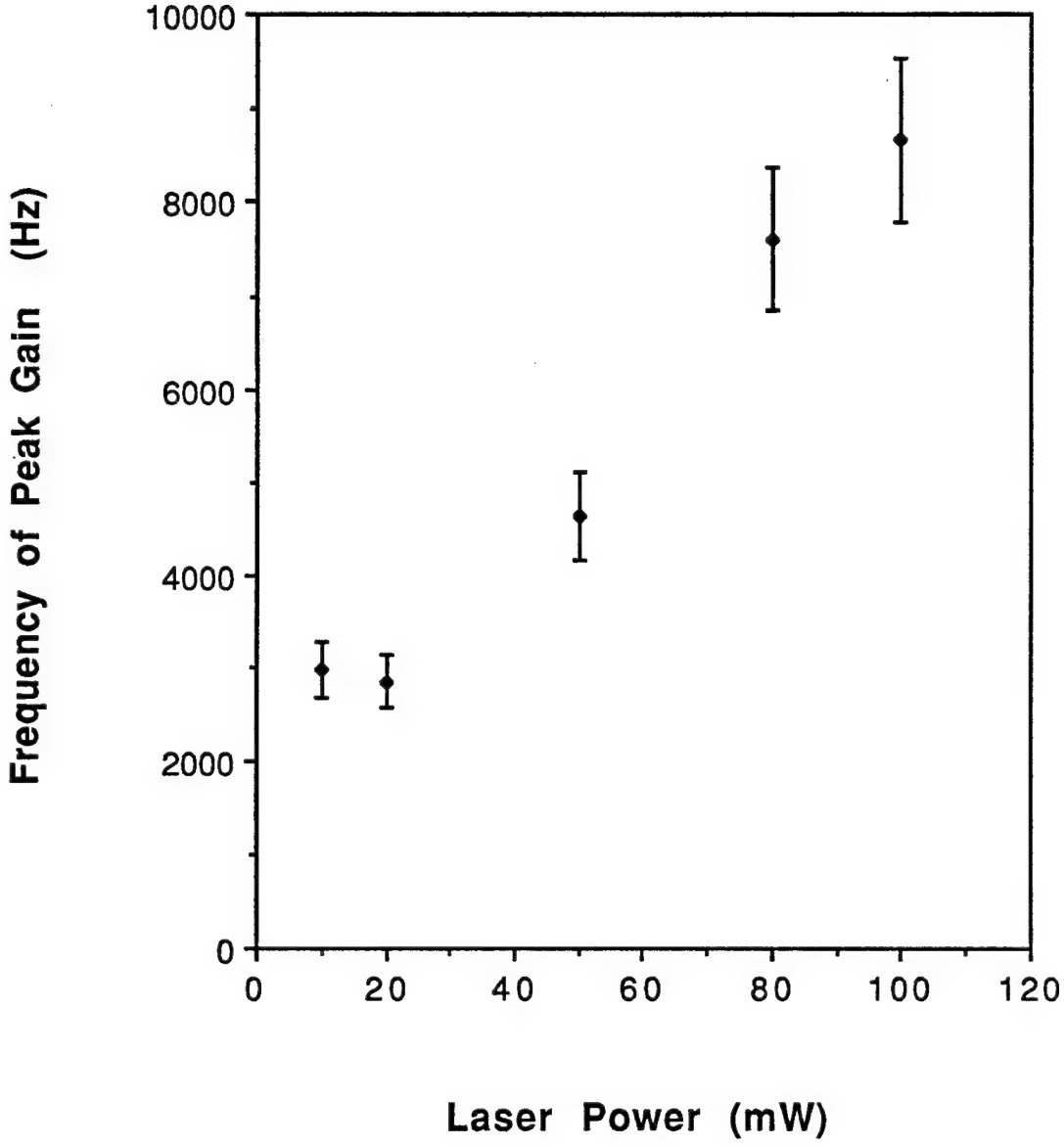
Frequency of Peak Gain (Hz)
10000
8000
6000
4000
2000
0
0
20
40
60
80
100
120
Laser Power (mW)

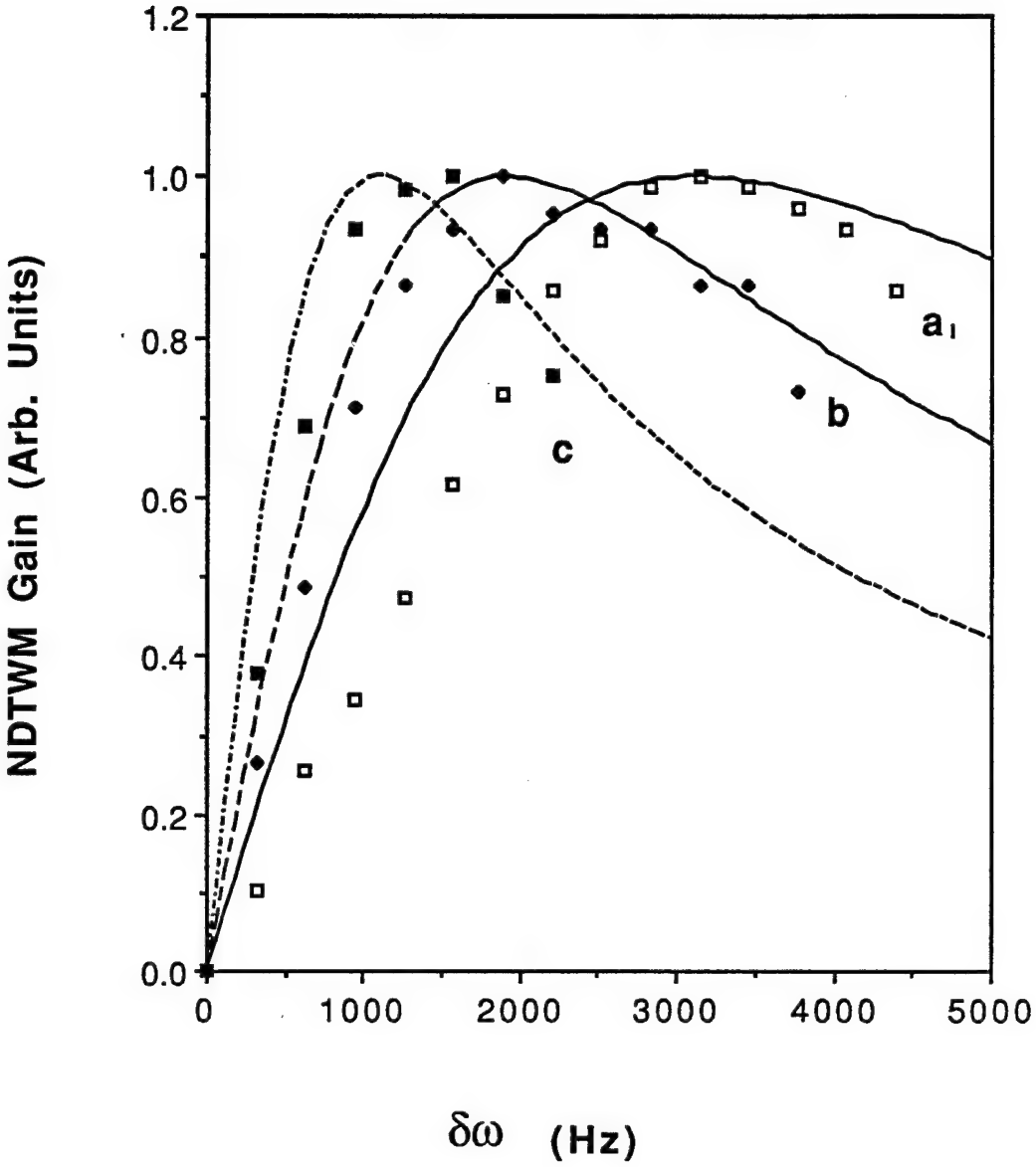
NDTWM Gain (Arb. Units)
1.2
1.0
0.8
0.6
0.4
0.2
0.0
0
1000
2000
3000
4000
5000
δω (Hz)
a1
b
c

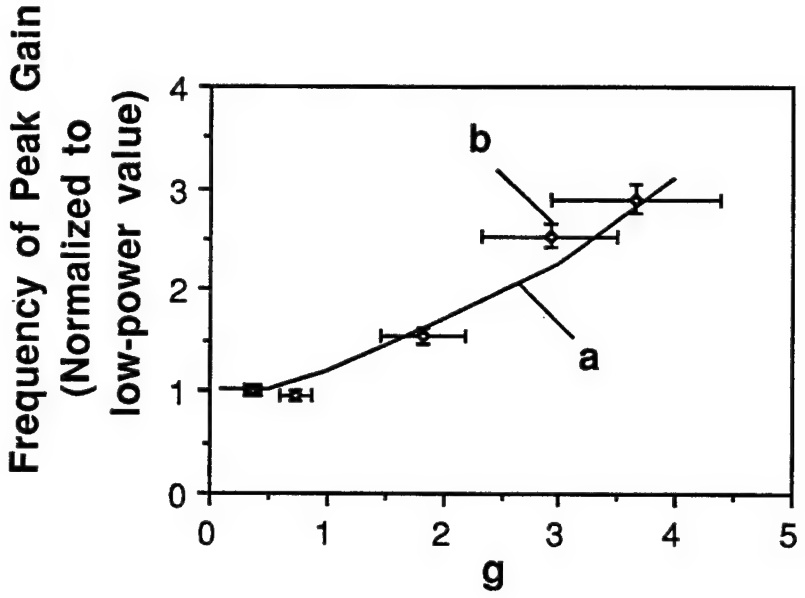
Frequency of Peak Gain
(Normalized to
low-power value)
4
3
2
1
0
0
1
2
3
4
5
g
b
a

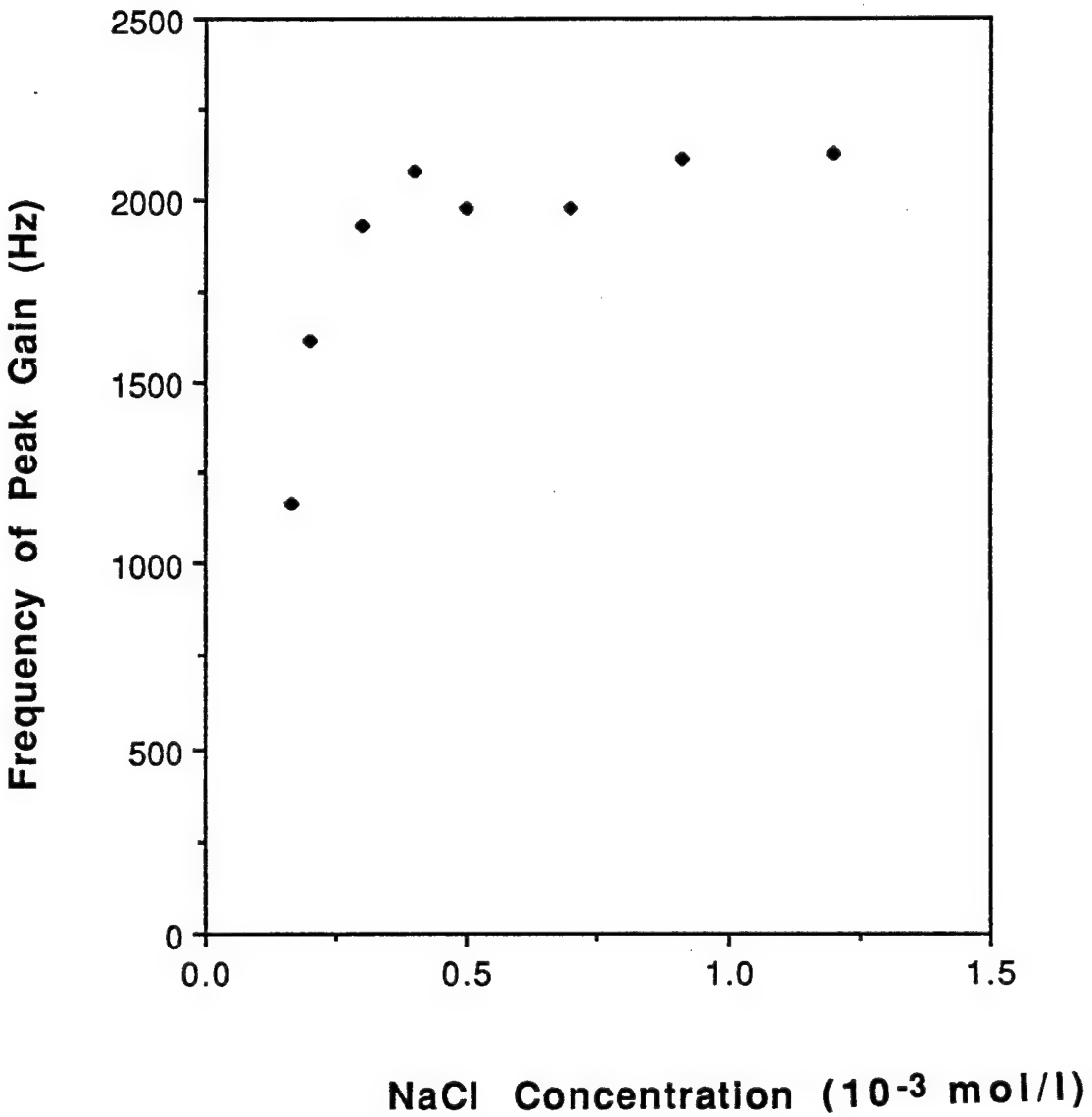
2500
2000
1500
1000
500
0
0.0
0.5
1.0
1.5
Frequency of Peak Gain (Hz)
NaCl Concentration (10-3 mol/l)

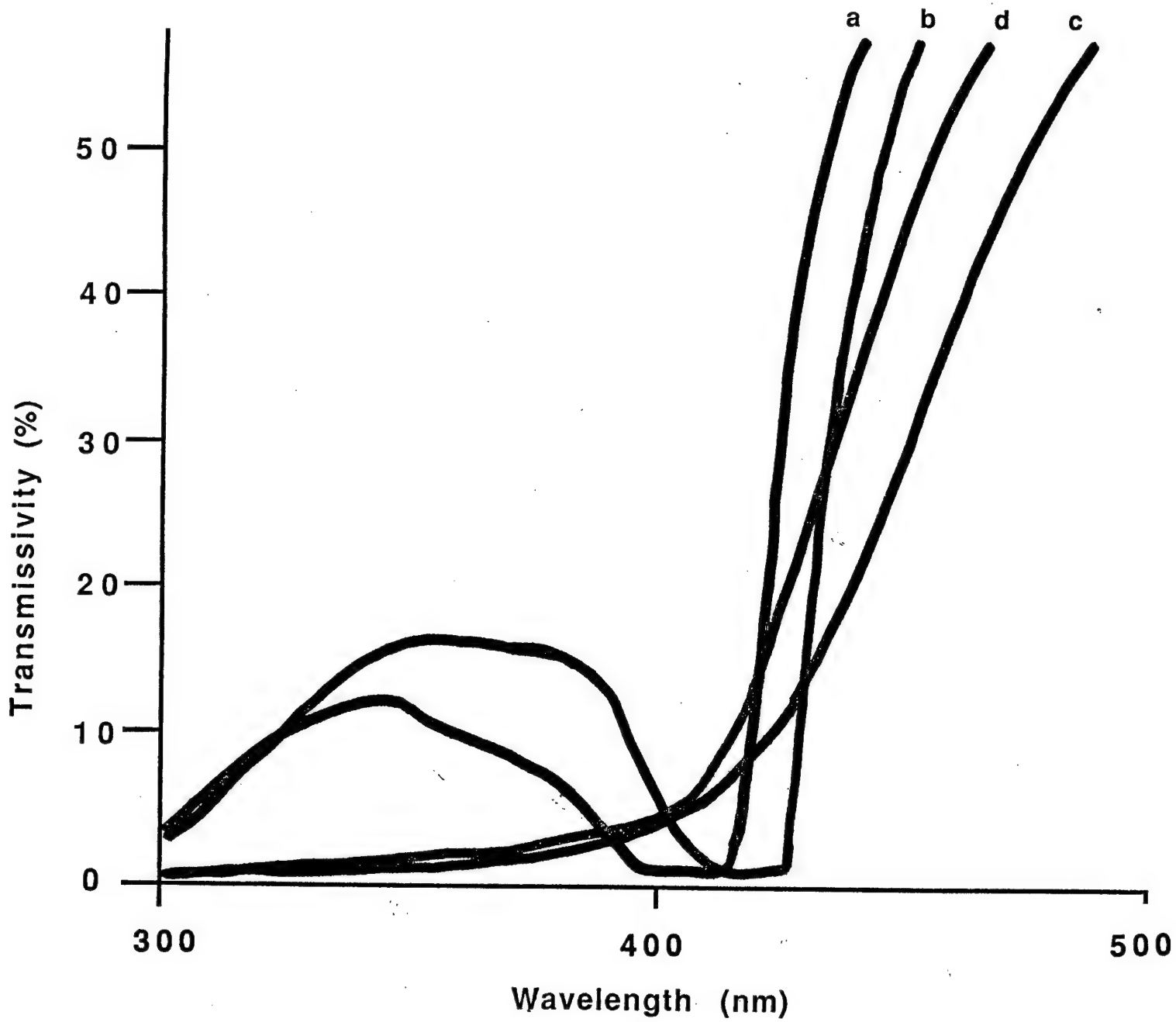
a
b
d
c
50
40
30
20
10
0
Transmissivity (%)
300
400
500
Wavelength (nm)

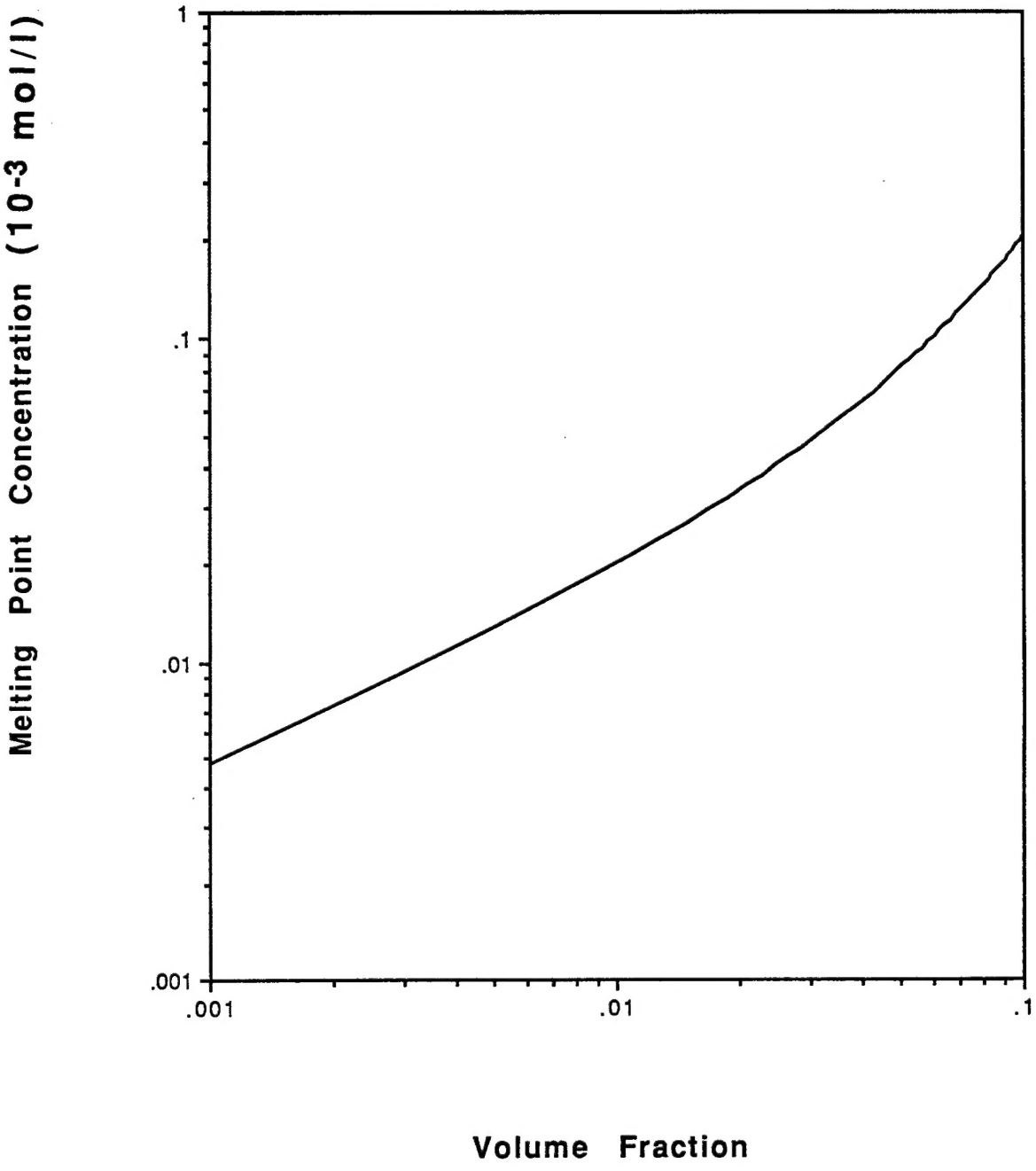
Melting Point Concentration (10-3 mol/l)
1
.1
.01
.001
.001
.01
.1
Volume Fraction

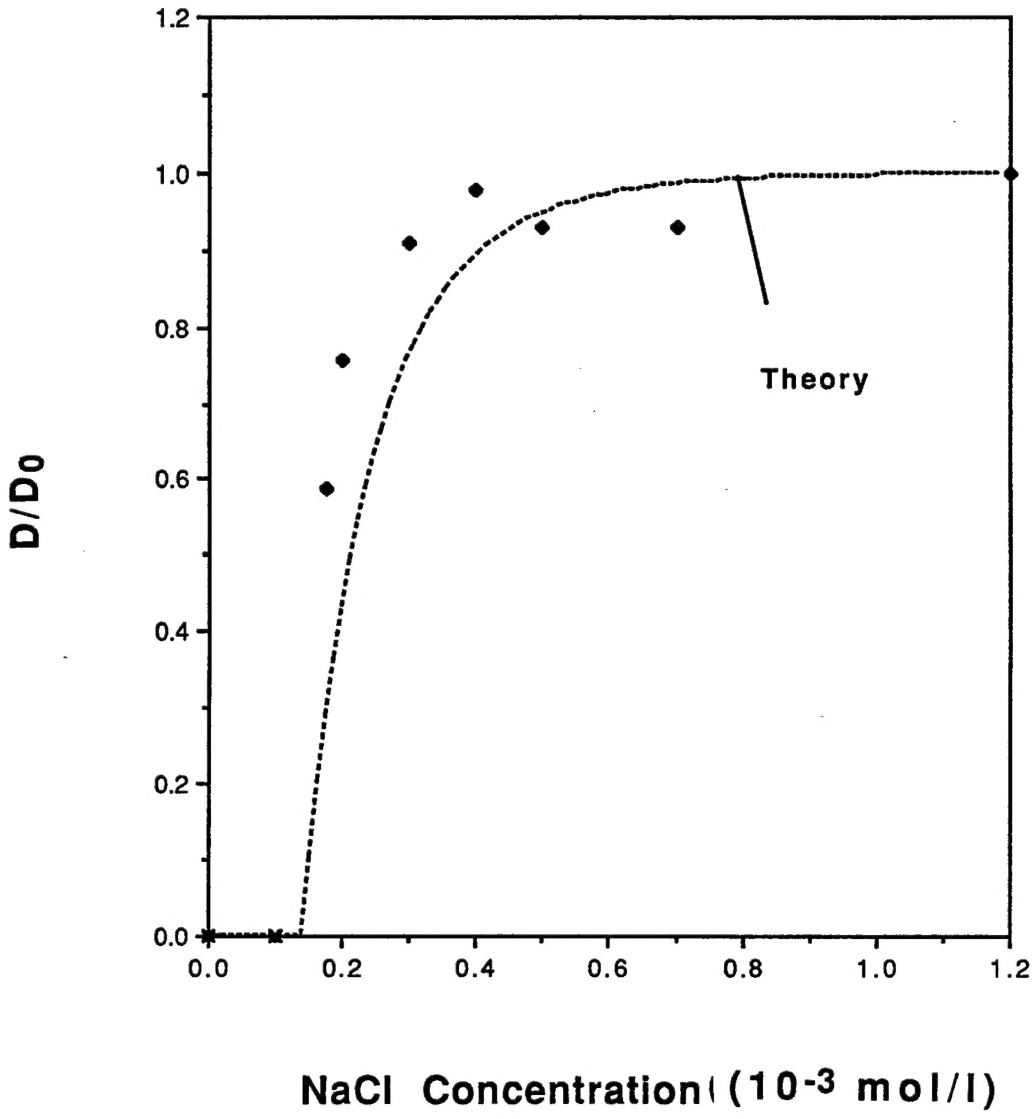
1.2
1.0
0.8
0.6
0.4
0.2
0.0
D/D0
Theory
0.0
0.2
0.4
0.6
0.8
1.0
1.2
NaCl Concentration (10-3 mol/l)

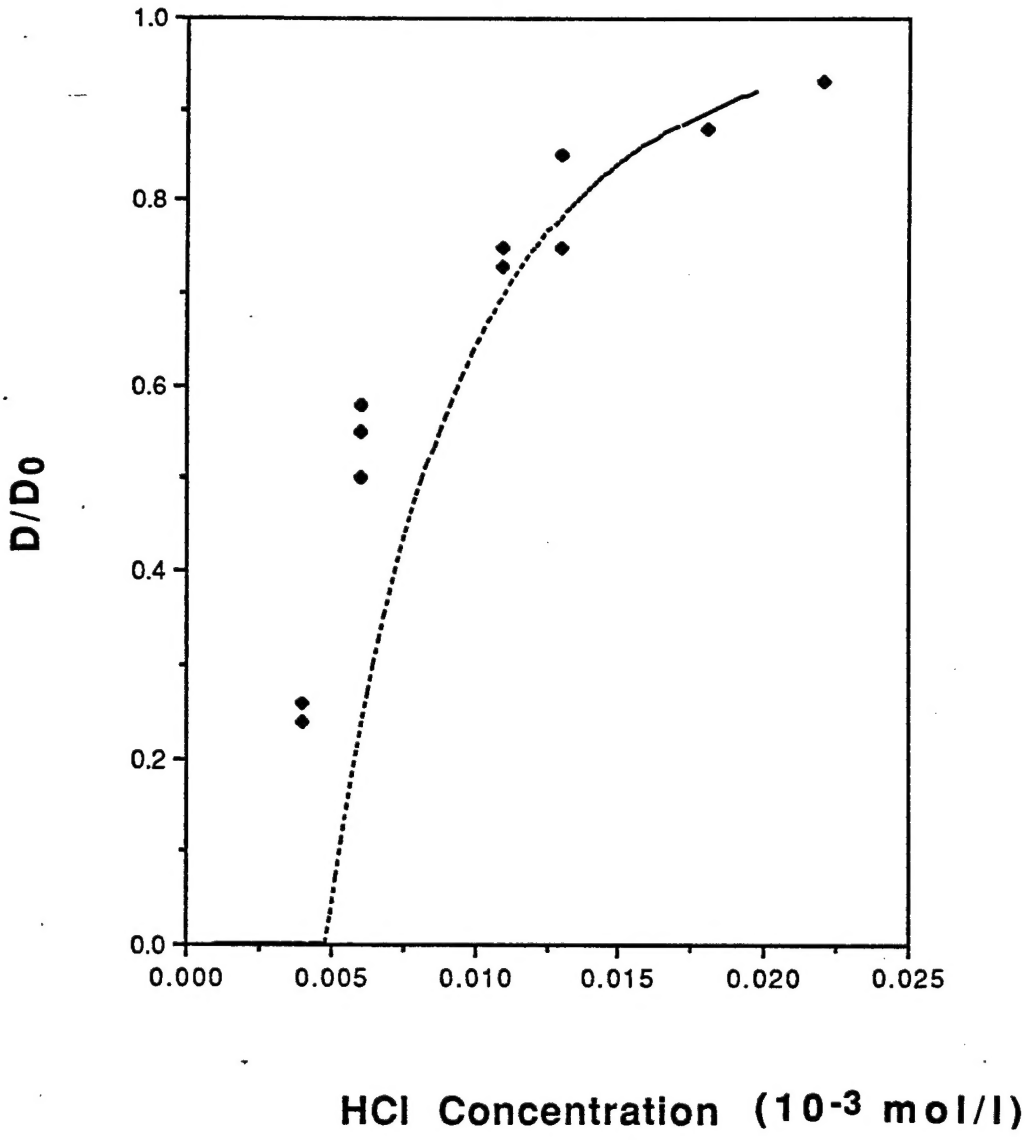
1.0
0.8
0.6
0.4
0.2
0.0
D/D0
0.000
0.005
0.010
0.015
0.020
0.025
HCl Concentration (10-3 mol/l)

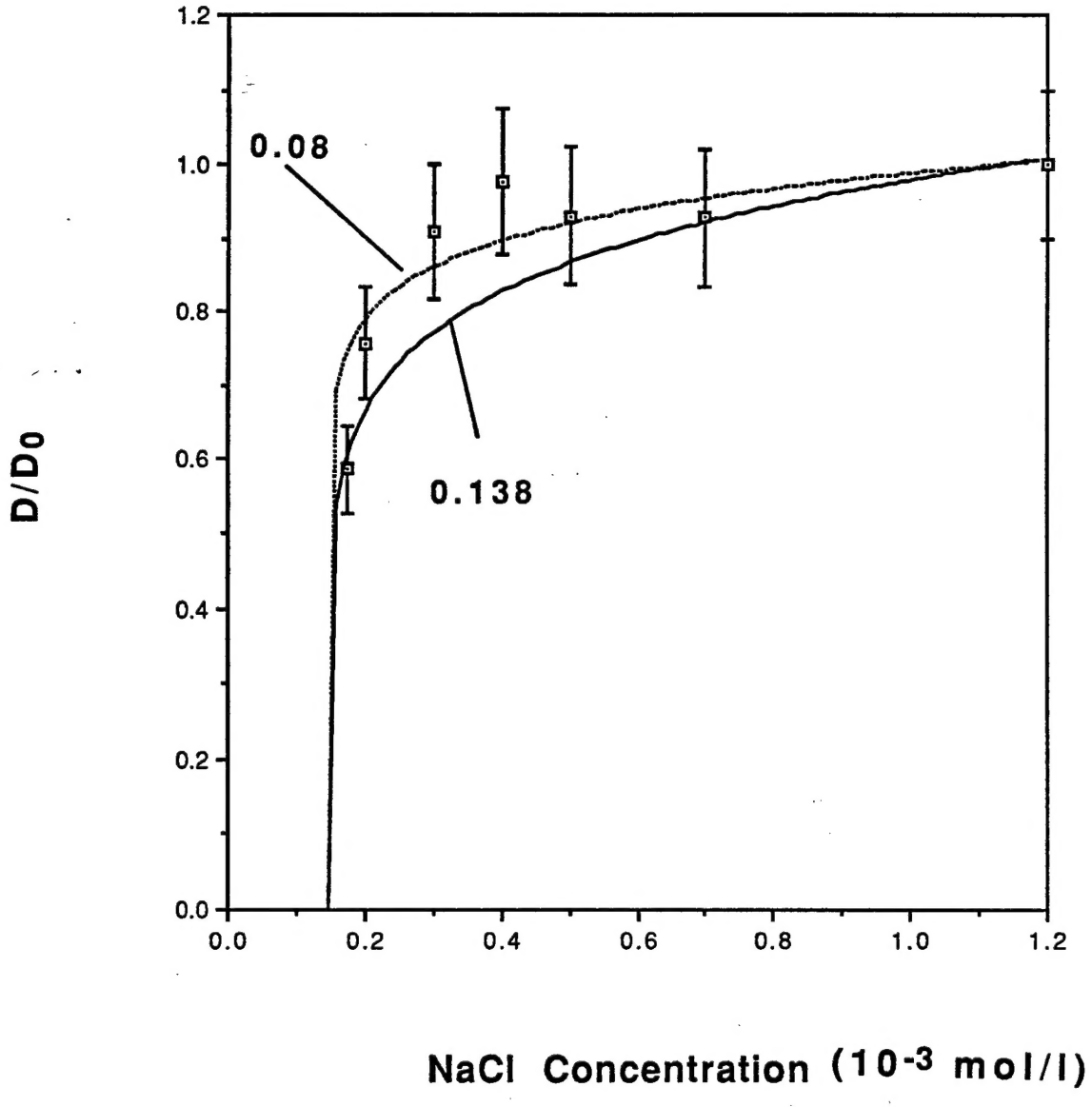
1.2
1.0
0.8
0.6
0.4
0.2
0.0
0.0
0.2
0.4
0.6
0.8
1.0
1.2
0.08
0.138
D/D0
NaCl Concentration (10-3 mol/l)